

Synthesis of $\text{Bi}_{0.5}\text{Na}_{0.5}\text{TiO}_3$ – BiFeO_3 solid solution via Combustion Synthesis Route

A THESIS SUBMITTED IN PARTIAL FULLFILLMENT OF THE REQUIREMENTS FOR
THE DEGREE OF BACHELOR OF TECHNOLOGY

By

SAMIKHYA JOSHI



DEPARTMENT OF CERAMIC ENGINEERING
NATIONAL INSTITUTE OF TECHNOLOGY
ROURKELA
2008-2009

Synthesis of $\text{Bi}_{0.5}\text{Na}_{0.5}\text{TiO}_3$ – BiFeO_3 solid solution via Combustion Synthesis Route

A THESIS SUBMITTED IN PARTIAL FULLFILLMENT OF THE REQUIREMENTS FOR
THE DEGREE OF BACHELOR OF TECHNOLOGY

By

SAMIKHYA JOSHI

(Roll : 10508007)

**Under the Guidance of
Prof. SUMIT KUMAR PAL**



**DEPARTMENT OF CERAMIC ENGINEERING
NATIONAL INSTITUTE OF TECHNOLOGY
ROURKELA
2008-2009**



**NATIONAL INSTITUTE OF TECHNOLOGY
ROURKELA
2009**

CERTIFICATE

This is to certify that the thesis entitled, **“Synthesis of $\text{Bi}_{0.5}\text{Na}_{0.5}\text{TiO}_3$ – BiFeO_3 solid solution via Combustion Synthesis Route”** submitted by **Miss Samikhya Joshi** in partial fulfillment of the requirements of the award of Bachelor of Technology Degree in Ceramic Engineering at the National Institute of Technology, Rourkela is an authentic work carried out by her under my supervision and guidance.

To the best of my knowledge, the matter embodied in the thesis has not been submitted to any other university / institute for the award of any Degree or Diploma.

Prof. Sumit Kumar Pal
Dept. of Ceramic Engineering
National Institute of Technology
Rourkela

Date: 13.5.09
– 769008

ACKNOWLEDGEMENT

First of all I express my sincere gratitude to Prof S.K.Pal for his support, his patience, his guidance, and his acceptance of me as a B.Tech student working under his guidance. I also want to thank my teachers Prof S.Bhattacharya, Prof J.Bera, Prof S.K.Pratihar, Prof B.B.Nayak, Prof R.Mazumdar and Prof A.Choudary for their encouragement, teaching and in helping me to successfully complete my B.Tech degree and also all the members of the technical staff of my department. I also want to thank Shyama Prasad Mohanty (M.Tech) for his help and guidance. Most of all, I deeply thank my family and friends who have been a constant support.

Date:13.5.09

Samikhya Joshi

CONTENTS PAGE NO.

A.ABSTRACT

i

B. TABLE OF CONTENTS

C.CHAPTER

1.	INTRODUCTION
1	

2.	LITERATURE	REVIEW
3		

3.STATEMENT	OF	PROBLEM
15		

4.	EXPERIMENTAL	PROCEDURE
		16

5.	RESULTS	AND	DISCUSSIONS
20			

6.	CONCLUSION
28	

D.REFERENCE
29

6.	CONCLUSION
27	

D.REFERENCE

Abstract:

$\text{Na}_{0.5}\text{Bi}_{0.5}\text{TiO}_3$ (NBT) and its modifications are known to be new lead-free piezo-ceramics materials and are promising candidates for environment friendly devices. An investigation was carried out on auto combustion synthesis of solid solutions $(1-x)\text{Na}_{0.5}\text{Bi}_{0.5}\text{TiO}_3$ [NBT] $-x\text{BiFeO}_3$ [BF] ($x = 0.04, 0.06, 0.08$). BNT-BF solid solution was prepared through citrate-nitrate solution combustion route. The pH of the precursor solution was maintain at 5 to 11 before combustion took place. All combustion products were calcined at 900°C for 2 hours to examine the effect of pH variation. A considerable change in crystallite sizes is observed with change in pH value.

LIST OF FIGURES :
NO.**PAGE**

Figure1: Representation of an ABO_3 perovskite shown as cubic BNT
2

Figure.2; Variation of the permittivity of the NBT–BF solid solutions as a
function of temperature at 250 kHz.
4

Figure3: Phase diagram for BNT with increasing mol % BT
8

Figure4: Phase relationship among BNT, BT and BKT near the MPB.
9

Figure5: Phase diagram of BNT with increasing strontium doping
10

Figure6.:Decrease in T_{max} of BNT with increasing mol % Sr
11

Figure7: Below is given the flow chart of the whole procedure
19

Figure8: XRD plot of 0.92BNT-0.08BF prepared at different pH
20

Figure9: XRD plot of 0.94BNT-0.06BF prepared at different pH
21

Figure10: XRD of 0.96BNT- 0.04BF prepared at different pH
21

Figure11: XRD peak of pure BNT with various amount of BF doping at pH 7.
22

Figure12:SEM of 0.92BNT- 0.08BF calcined powder
25

Figure13:SEM of 0.92BNT-0.08BF sintered pellets
25

Figure14: SEM of calcined powder of 0.94BNT-0.06BF
26

ii

Figure15: SEM of sintered pellets of 0.94BNT-0.06BF
26

Figure16: SEM of 0.96BNT-0.04BF sintered pellets
27

LIST OF TABLES : NO.

PAGE

Table 1: Phase Transitions in BNT Measured by Jones

Table 2: Crystallite size of the samples.
23

Table 3: Density measurement of sintered pellets
24

1. Introduction:

Piezoelectricity is a property of certain crystalline materials. When a mechanical force is applied to these materials an electric field proportional to the magnitude of the stress is produced. Conversely, when an electric field is applied to a piezoelectric, a mechanical stress develops that may produce a shape change.

The underlying mechanism behind piezoelectricity is an asymmetry in the unit cell of the materials. Piezo materials contain domains, i.e., regions which possess a spontaneous electric polarization. When subjected to an external electric field, these domains can reverse their orientation and this behavior is the defining characteristic of piezoelectrics.

There are several piezoelectric materials that are used in electromechanical sensors and actuators. Some examples of practical piezo materials are barium titanate, lithium niobate, polyvinylidene difluoride (PVDF), and lead zirconate titanate (PZT).

Lead free piezoceramics:

Lead has recently been expelled from many commercial applications and materials (for example, from solder, glass and pottery glaze) owing to concerns regarding its toxicity. Lead zirconium titanate (PZT) ceramics are high-performance piezoelectric materials, which contain more than 60 weight per cent lead. It becomes necessary to develop lead-free piezoelectric materials with properties close to those of the PZT system ¹. In this regard $\text{Na}_{0.5}\text{Bi}_{0.5}\text{TiO}_3$ compound (NBT) is considered as a possible candidate for such applications.²

Bismuth sodium titanate is an ABO_3 distorted perovskite with an rhombohedral $R3c$ crystal structure at room temperature.¹⁹ The standard ABO_3 perovskite formula for BNT is $(Bi_{0.5}Na_{0.5})TiO_3$. An ABO_3 perovskite can be considered in two ways; one way is to have the bismuth and sodium cations occupy the corners of a cubic unit cell, oxygen cations occupying the face centers, and a titanium cation in the center of the oxygen octahedra that is formed. The other way, is a three-dimensional cubic network of 8 corner-sharing TiO_6 octahedra with bismuth and sodium cations at

1

the center of the cube formed by the octahedra.²⁰ Figure 1 represents a typical ABO_3 perovskite, shown here as cubic BNT. The figure suggests that the bismuth and sodium ions are ordered on the A site of the structure; this is only to show the stoichiometry that is present in an ideal mixture. The real material does not exhibit any long range ordering as described later in the text.



Figure 1: Representation of an ABO_3 perovskite shown as cubic BNT

NBT has large polarization, high temperature dielectric constant and also no lead so it can be developed to be used as future replacement for all lead based compounds. But pure NBT has a drawback of high coercive field, $E_c = 7.3$ kV/mm and the high conductivity causes problems during the poling process.¹ To improve the properties some doping has to be done such as NBT–BaTiO₃, NBT–PbTiO₃, NBT–K_{0.5}B_{0.5}TiO₃, NBT–SrTiO₃ and NBT–BiFeO₃.³⁻¹¹

In the present work BNT-BF solid solution has been synthesized with BF with gradual increase in doping concentration.

2. Literature Review:

Ferroelectric perovskite-type compounds with different distributions of the 6- or 12-fold coordination cations are more and more being increased as these materials are involved in the fabrication of many devices, e.g. capacitors, piezoelectric ultrasonic transducers, electrostrictive actuators, SAW substrates, etc.⁽¹²⁻¹⁴⁾ These materials have indeed high electromechanical characteristics which can be controlled either by doping or compositional change. The latter is connected in some cases with the onset of cationic disorder, the magnitude of which strongly influences the properties, mainly due to the dependence of the nature of the phase transition on the cationic distribution.¹⁵

The commonly used materials are lead based eg-lead zirconate titanate (PZT), lead magnesium niobate (PMN), etc. However, the toxicity of lead oxide and its high vapor pressure during the sintering process results in serious environment problems. As a consequence, it becomes necessary to develop low-lead or lead-free piezoelectric materials with properties close to those of the PZT system.¹ Because of environmental issues, new lead-free piezoelectric materials are the object of many studies. The $\text{Na}_{0.5}\text{Bi}_{0.5}\text{TiO}_3$ compound (NBT) is considered as a possible candidate for such applications.² BNT has large polarization, high temperature dielectric constant and also no lead so it can be developed to be used as future replacement for all lead based compounds. But pure NBT has a drawback of high coercive field, $E_c = 7.3 \text{ kV/mm}$ and the high conductivity causes problems during the poling process¹

To improve the properties some doping has to be done such as NBT–BaTiO₃, NBT–PbTiO₃, NBT–K_{0.5}B_{0.5}TiO₃, NBT–SrTiO₃ and NBT–BiFeO₃.³⁻¹¹

NBT–BF system behaves in a different way with respect to the two previous ones. Two ranges of compositions can be distinguished. For BF content $\leq 50 \text{ mol.}\%$, the overall behaviour of the permittivity is similar to that observed for low substituted NBT (Fig 2 top) but the local maximum is shifted towards higher temperatures as the BF content increases. This can be connected with the high Curie temperature of BiFeO₃. For BF content $> 50 \text{ mol.}\%$, the maximum of the permittivity has disappeared, but an additional maximum occurs at high temperatures between 600 and 750 °C (Fig. 2 bottom). The substitution of Fe³⁺ for Ti⁴⁺ has an influence not only on the structural characteristics

but also on the electromagnetic behaviour as Fe³⁺ has a *d*⁵ electronic configuration, with a finite magnetic moment (in contrast, Zr⁴⁺ and Sc³⁺ are spherical ions with non-magnetic *d*⁰ configuration). It is therefore reasonable to infer that this anomalous behaviour would be somewhat connected with the magnetic character of the BF-rich materials. In addition, as the ceramics become more conductive for high BF contents, one cannot neglect the presence of mixed-valence (Fe²⁺ /Fe³⁺) cations, which might influence the high dielectric behaviour. Further investigations about this problem are now in progress.¹

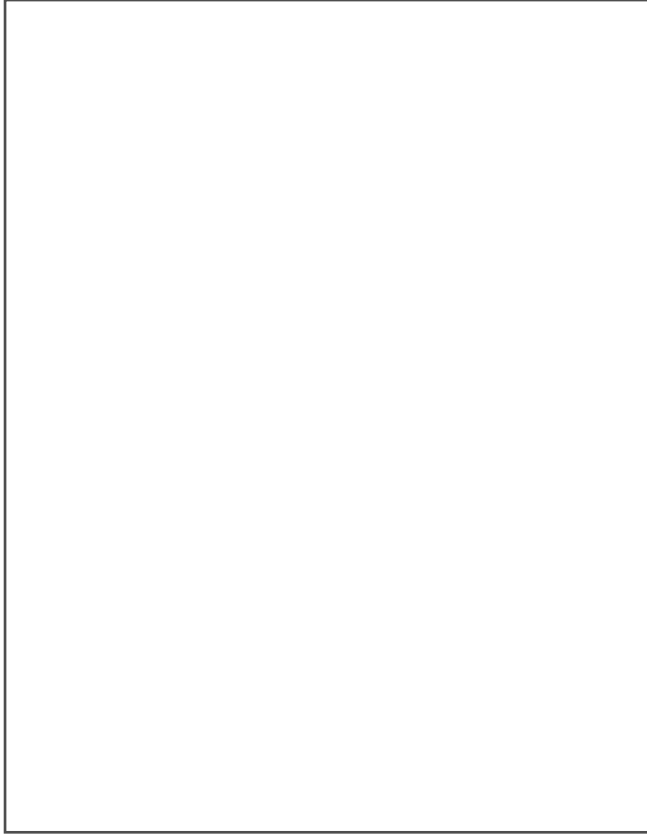


Figure 2: Variation of the permittivity of the NBT–BF solid solutions as a function of temperature at 250 kHz.

2.1 Structure of BNT-

Many structural investigations have been performed on BNT since it was discovered in 1960 by Smolenskii et al. These studies used the best methods of the time to determine the phases and phase transitions of BNT.^{15,21-26} Phase transitions determined from these earlier studies have since

4

been clarified by an extensive neutron powder diffraction study of BNT. This study definitively determined the phase transitions and crystal structures at various temperatures (Jones and Thomas, 2002). The results of this study are shown in Table I. As the table shows, with decreasing temperature, BNT transforms from cubic Pm3m to tetragonal P4bm and then to rhombohedral R3c with coexistence regions between them. These phase transitions are important to the electrical properties of the material because only non-centrosymmetric space groups can exhibit ferroelectricity.

The rhombohedral R3c space group is polar with parallel cation displacements along the $[111]_p$ pseudo cubic direction along with antiphase a-a-a- oxygen octahedral rotations. Thorough explanations of the types of octahedral tilting and the associated mechanisms are available to more fully understand this phenomenon (Woodward 1997).^{20,27} Cation displacements along with octahedral rotations allow the crystal to have a

spontaneous polarization (P_s); polarization is necessary for a material to be ferroelectrically active.

The tetragonal $P4bm$ phase is also a polar phase, although it has a weaker polarization response than the $R3c$ phase. The oxygen octahedra in the tetragonal phase exhibits $a0a0a$ -rotation behavior about the c axis with anti-parallel cation displacements of A-site cations along the polar c -axis.^{19,28} The tetragonal phase distortion produces a weaker polarization response because the atomic displacements are less than those in the $R3c$ phase. Smaller atomic displacements result in a lower polarization in the material. This is evident by the decrease in relative permittivity above the Curie temperature(320°C).

Table I: Phase Transitions in BNT Measured by Jones and Thomas, 2002.



Phase transitions in ferroelectric materials are one of the main parameters that need to be controlled to tailor the properties to meet specific applications. Phase transitions are one of the main determinants of the dielectric properties of the material. Compositional additions to the BNT structure can be chosen to modify the phase transitions that occur within the material at various temperatures. Dopants are selected to change specific characteristics of the phases such as relative permittivity, Curie temperature (T_c), relative permittivity peak height and number of phase transitions. The Curie temperature is the temperature where the relative permittivity of the material is the largest. This usually occurs where there is a phase transition. Some materials, such as BaTiO_3 , exhibit Curie Weiss behavior as discussed before, while others undergo a diffuse phase transition.

Bismuth sodium titanate is a relaxor ferroelectric in the rhombohedral phase and it exhibits diffuse phase transitions between each of the phases. Diffuse phase transitions are described by a coexistence region between phases as discussed above. Diffuse phase transitions are evident in the dielectric response because the relative permittivity peaks become broad instead of having a sharp peak, like those seen in materials with Curie Weiss behavior. Broad relative permittivity peaks are most prominent in solid solutions and in disordered structures. The Curie range, rather than the Curie temperature can be used to describe the broad peaks that are created by the diffuse phase transitions.

The temperature range will typically vary with the frequency used in the measurement. The breadth of the phase transition depends mostly on the amount of disorder in the structure. Largely disordered structures will have a wider peak than those with less disorder. Each compositional fluctuation in the material will exhibit its own peak dielectric constant. These individual units combine together to form a broad peak that is composed of many smaller compositional peaks. If each compositional unit had a peak K at different temperatures, the material peak would extend over the range of temperatures of the individual units. This broad peak can be thought of as a global average of the peaks created by the individual disordered

units. The disordered material basically acts like a composite matrix where each section has an effect on the overall properties of the matrix.²⁹

2.2 Effect of dopants:

Many studies have been performed on BNT to determine how dopants affect the structural and electrical properties of the material. Some studies focus on dielectric properties, while others focus on piezoelectric properties. BNT is a good material for both applications because it can be modified to enhance a specific desirable behavior. Both A-site and B-site dopants have been studied to determine how they affect the properties of BNT, some of these dopants include (Ba, Pb, Sr, Zr, La, K, Bi).^{15,18,22,23,25,30-46}

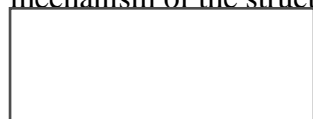
Attfield, 2002 states that the properties of ABO_3 perovskites are mainly controlled by the B-site cations; however, the properties of the material are tuned by the cation(s) on the A-site.⁴⁷ This statement is somewhat misleading because the properties can be tuned by both A and B-site doping. The main characteristics of the perovskite must be determined on an individual basis for a more accurate assessment of the ferroelectric properties. Some materials are distorted on the A-site as in BNT, while others such as BT, exhibit B-site distortion. A-site distortion in BNT is created by the valence deficiency of the Bi^{3+} and Na^+ ions, along with their ionic size compared to the space that is available in the structure.

For many years, the Goldschmidt tolerance factor calculation has been used to determine the stability of perovskites. This calculation, given by Equation 1, only considers ionic size to determine the type of perovskite that will form. This method is limited in its use because it only gives a range of

7

values for which a mixture of ions will form a stable structure. It also gives a vague range that could

help to determine if the structure will be ferroelectric (FE) or antiferroelectric (AFE). It does not give any information regarding the type of distortion that will take place in the structure. Over the years, tolerance factor ranges have been determined to describe the typical behavior of a material in that range. On the other hand, the bond valence tolerance factor, discussed later in the text, uses the valence of the ions along with other variables to determine the distortion mechanism of the structure.



-----Eq-1

Where: R_A is the ionic radii of the A-site cation

R_B is the ionic radii of the B-site cation

R_x is the ionic radii of the anion

The typical range for stable perovskite mixtures is between $0.78 \leq t \leq 1.05$ for VI and XII coordination and Shannon-Prewitt radii. This range is limited in its predicative value because it has been found that AFEs range from $0.78 \leq t \leq 1.00$, and that FEs can be found throughout the full range.⁴⁸ Other tests must be performed to confirm the behavior of the material.

2.2.1 Barium doping in BNT:

The effects of barium on the properties of BNT have been characterized by various groups over the years. Many studies that involve barium doping also include another A or B-site cation to evaluate the effects of multiple-site doping on the properties.^{18,30,32-34,38} One of the advantages of doping with barium is that there is a morphotropic phase boundary (MPB) between the rhombohedral and tetragonal phases of the structure. Dielectric materials near an MPB are interesting because they exhibit anomalously large dielectric constant values compared to other compositions. BNT doped with barium has been shown to exhibit an MPB near 7 mol % Ba. The compositions near this value exhibit a large, broad dielectric constant peak. The broad peak is a result of the MPB behavior, along with increased disorder created by the Ba²⁺ ions that substitute for the Bi³⁺ and Na⁺ ions on the A-site. As discussed earlier, diffuse phase transitions present in relaxor ferroelectrics are caused by increased disorder in the structure. Figure 3 shows a phase diagram for a solid solution between BNT and BT with increasing BT mol %.³²

8



Figure 3: Phase diagram for BNT with increasing mol % BT.³²

Doping BNT with multiple cations is another way to modify the structure to obtain results that could not otherwise be obtained by single dopant modifications. Sheets et al. simultaneously doped BNT with Ba²⁺ and Zr⁴⁺ ions to stabilize the AFE phase to near room temperature. This is important because the peak that is created is very broad with a stable relative permittivity over a large temperature range. They also determined that the behavior between single crystal samples, and polycrystalline samples of the same composition were virtually identical; except, the single crystal sample had a larger value of relative permittivity.³⁰ This behavior is to be expected in a dielectric material because a single crystal is free of defects such as cracks, voids and grain boundary effects that will combine to reduce the overall relative permittivity of a polycrystalline sample.

Li et al. reported that doping with 6 mol % Ba and 1 mol % each of La³⁺, Co³⁺ or Nb⁵⁺ will modify the dielectric response compared to BNT doped with 6 mol % Ba. Each of the dopants reduced the value of the relative permittivity and some enhanced the intermediate phase transition referred to as a ‘shoulder’ in some articles. The addition of La³⁺ also produced smaller grain sizes than the other dopants.³³

Nagata et al. reported on the properties of BNT with the addition of both BaTiO_3 and $(\text{Bi}_{0.5}\text{K}_{0.5})\text{TiO}_3$ (BKT). They reported that an MPB exists at a composition containing 85.2% BNT, 2.8% BaTiO_3 and 12% $(\text{Bi}_{0.5}\text{K}_{0.5})\text{TiO}_3$. Figure 4 shows the phase relationship near the MPB for the

9

BNT/BT/BKT multi-component system. They found that the most useful compositions were located

near the MPB because they exhibited the anomalous electrical behavior associated with MPB compositions.³⁸



Figure 4: Phase relationship among BNT, BT and BKT near the MPB.³⁸

2.2.2 Strontium doping in BNT:

Strontium doping in BNT has a well defined effect on the dielectric properties of the material. Sr^{2+} ions can substitute for both Bi^{3+} and Na^{+} ions on the A-site of the perovskite because the average valence between the Bi and Na ions is 2+. Figure 5 shows a phase diagram created in 1974 for BNT doped with SrTiO_3 (ST).²³

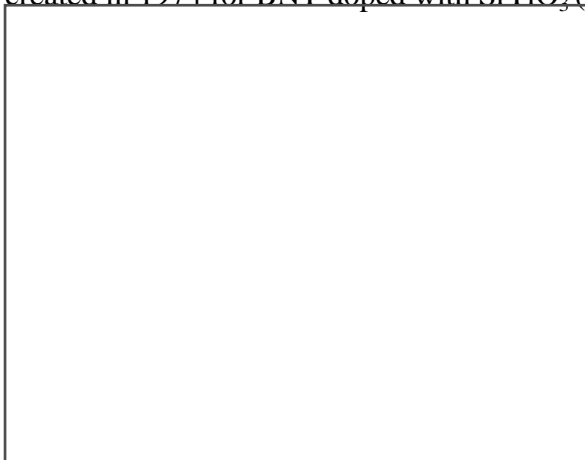


Figure 5:Phase diagram of BNT with increasing strontium doping.²³

10

It has been reported that BNT doped with SrTiO_3 (ST) exhibits an MPB in the range of 26-30 mol %.²⁰ The MPB is shown in the phase diagram in Figure 5 above, because there is a tetragonal antiferroelectric region (AFE) between the ferroelectric rhombohedral and paraelectric cubic phases up to about 50 mol % ST. The MPB theory is bolstered by the dielectric measurements because the compositions with 26-30 mol %

ST show enhanced dielectric properties with a broad peak, as discussed earlier for MPB behavior. It has been reported that instead of having an MPB, strontium doped BNT exhibits a very large diffuse phase transition region between 26 mol % ST and 50 mol % ST.^{22,34} The large temperature range over which the peak K spreads suggests that the diffuse phase transition may be a more reasonable explanation. Park et al. suggests that within the 26-50 mol % region, there are non-uniform units of polarized material within a matrix of non-polarized material.

To explain this point further, in tetragonal structures there are six possible polarization directions. The polar units in the matrix may adopt any of the six directions unless the material has been poled in a specific direction. Thermal energy causes the polar units to vibrate and therefore not maintain a specific direction. If each polar unit does not have a negative counterpart, the material will have a net polarization in a given direction. This net polarization is the cause of the weakly polar structure found in the 26-50 mol % region of strontium doped BNT.⁴⁹

In general, as the amount of Sr^{2+} increases, the dielectric constant peak will increase in value, and shift to lower temperatures. Increasing Sr content also decreases the lattice distortion of the material; this behavior is predicted by the bond valence model discussed later in the text. The peak temperature decrease has been shown to decrease in a highly predictable linear manner.²² Figure 6 shows the linear nature of the decrease in peak temperature of BNT as the amount of strontium is increased. The slope of the line is reported to be $-5.3^\circ\text{C}/\text{mol}\%$. The linear nature depicted in the figure is advantageous for tuning the peak temperature to a specific value.

11



Figure 6:Decrease in T_{\max} of BNT with increasing mol % Sr.²²

2.2.3 Doping that causes peak suppression in BNT:

One element that has been used for peak suppression in PZT is tin (Sn^{4+}). Tin is used as a substitute for zirconium or titanium on the B-site in PZT to stabilize the antiferroelectric phase of the material. Feng et al. discovered that as the amount of Sn was increased in PZT, the main dielectric constant peak became more diffuse, and reduced in value along with a slight shift to lower temperatures. Their results for relative permittivity versus temperature showed that the peak temperature reduced slightly and that the peak was suppressed as the amount of tin dopant increased.^{50,51}

Nagata et al. discovered that with the addition of BiScO_3 , the main dielectric peak in BNT will become more diffuse; as a result, peak suppression will occur. Extra bismuth ions were added because it was concluded that the ferroelectricity of BNT was mainly caused by the Bi^{3+} ions on the A-site of the structure. Therefore, they did not want to remove Bi^{3+} ions by substituting them directly with Sc^{3+} ions. The relative permittivity versus temperature results for these additions showed that as the amount of BiScO_3 increased, the permittivity peak was suppressed.¹⁵

2.2.4 Lead doping in BNT:

The use of lead in electronic ceramic materials has been common over the years because of the good properties that lead provides. The lone pair characteristics associated with lead creates ions that are capable of large polarizations in materials. The large amount of polarization is useful for synthesizing materials with a high permittivity, and a large electromechanical response in piezoelectric materials.

12

The problem with lead is that it is not environmentally friendly; being that it is fairly toxic to living organisms. Special care must be taken when handling lead in its many forms to prevent any contamination of the worker or the environment.

Lead Pb^{2+} doping on the A-site in BNT is useful because it boosts the relative permittivity, and enhances the response of the intermediate phase transition that occurs near 200°C . BNT compositions doped with lead have been reported to exhibit an MPB anywhere between 12-18 mol %.^{24,31,36}

BNT modified by lead has also been modified on the A-site with dopants like K^+ , La^{3+} on the A-site, and on the B-site with Zr^{4+} .^{25,36,37,52} The addition of K^+ ions to BNT with lead causes an extension of the intermediate phase, and an increase in the relative permittivity. Lanthanum additions shift all of the phase transitions to lower temperatures and reduce the relative permittivity. BNT doped with Pb^{2+} and Zr^{4+} ions has a more diffuse phase transition, which creates a very broad relative permittivity peak.

2.2.5 Other dopants in BNT:

There are many other elements and combinations of elements that can be used for doping BNT to modify its properties. One such element of interest is lanthanum La^{3+} , because it restricts grain growth and enhances densification.⁴³ One of the disadvantages is that it decreases the magnitude of relative permittivity at room temperature because it is replacing a more polarizable ion in Bi^{3+} . Lanthanum doping enhances the shoulder that appears near 200°C , and broadens the high temperature peak. The peak broadening has been attributed to increased lattice distortion caused by the strain created when La^{3+} ions replace Bi^{3+} ions on the A-site of the structure.⁴⁴ Herabut and Safari performed x-ray diffraction on the La doped samples to determine the lattice parameters of each sample and to determine the phase of each sample. The authors

determined the lattice

parameters for La doping levels between 0-6 mol %. They found that a phase transition between rhombohedral and cubic would occur near 2-5 mol % La additions.⁴²

Another area of interest for BNT doping is with solid solution compounds containing potassium K^+ ions. Compounds such as $Bi_{0.5}K_{0.5}TiO_3$ (BKT) and $KNbO_3$ (KN) are of interest because of the MPB behavior that they exhibit. The solid solution of BNT-BKT has been found to have an MPB between the rhombohedral and tetragonal phases in the range of 16-20 mol % BKT.³⁹ This is significant because of the enhanced electrical properties that MPB compositions exhibit. The

13

solid solution of BNT-KN has been found to contain an MPB between the rhombohedral and orthorhombic phases in the range of 94-97 % KN. These results were determined by Ishii et al. and their results can be found in the literature.⁴⁰

3.Statement of Problem:

1. Develop BNT-BF solid solution by citrate – nitrate solution combustion synthesis route.
2. To observe the variation of pH on powder prepared by combustion synthesis route
3. XRD analysis for phase identification
4. Sintering of powder compact
5. Density measurement and SEM analysis

4. Experimental Procedure:

4.1 The raw materials used for synthesis of BNT :

- Bismuth nitrate ($(\text{Bi}(\text{NO}_3)_3) \cdot 5\text{H}_2\text{O}$, Analytical Rasayan, AR)
- Sodium nitrate (NaNO_3 , Qualigens)
- Iron nitrate ($\text{Fe}(\text{NO}_3)_3$, Merck)
- Titanium dioxide (TiO_2 , Merc)
- Conc. Sulphuric acid (conc. H_2SO_4 , Merck)
- Ammonium sulphate ($(\text{NH}_4)_2\text{SO}_4$, Merck pure 99%, GR)
- Hydrochloric acid (HNO_3 , Merck pure 67%)
- Ammonium hydroxide (NH_4OH , Merck pure 25%)
- Citric acid (Merck)

4.2 Preparation of iron nitrate solution:

5gm of iron nitrate was dissolved in 50 ml of distilled water. Then in a 250 ml volumetric flask the volume was made up and the flask was shaken. The solution was filtered through Whatman-42 filter paper to remove any impurity and the clear solution was collected. 3 ml of this clear solution was taken individually in two 50 ml beakers. To it 2-3 drops of AAC buffer was added to get a precipitate. This is then filtered through Whatman-40 filter paper along with washing with hot water. Then the precipitate collected was taken in a pre weighed platinum crucible and kept in furnace to be fired at 1000°C for 1 hour. After firing the platinum crucible were again weighed and the differences in the previous weights and now gives the amount of iron oxide present in 50 ml of iron nitrate solution.

4.3 Preparation of Ti-Oxynitrate solution:

10 gm of TiO_2 was mixed with 150 ml of conc. H_2SO_4 and 70 ml $(\text{NH}_4)_2\text{SO}_4$ and heated till a clear and transparent solution was obtained. The solution was then cooled and its volume doubled. Now NH_4OH was added to get precipitate. The pH was maintained at 10. The solution was allowed to settle down and then decantation was done till all the ammonia was removed. It was then centrifuged and washed. 1:1 HNO_3 was added to the precipitate obtained and solution was prepared. Then it was filtered and to 10 ml of the solution NH_4OH was added to get a precipitate. Then filtration was done and the residue was taken in a pre weighed platinum crucible and fired at 900°C for 1 hour. The crucible was then weighed and the difference between earlier weight and new weight gives the

16

amount of titania present in 10 ml of the solution.

4.4 Powder preparation by combustion synthesis:

Combustion synthesis method was adopted to produce powder for samples. $(1-x)\text{NBT}-x\text{BF}$ was prepared with $x=0.02, 0.04, 0.06$. For powder preparation bismuth nitrate ($\text{Bi}(\text{NO}_3)_3 \cdot 5\text{H}_2\text{O}$) powder, sodium nitrate (NaNO_3) powder, titania solution, iron nitrate solution were used. The chemicals were taken in a beaker according to stoichiometric proportions. Then the pH varying from 5, 7, 9, 11 was achieved by adding required amount of ammonium hydroxide solution. Stoichiometric proportion of citric acid was added as fuel. Then the combustion synthesis was carried out on a hot plate. The powder was scraped and collected. Also a pure BNT sample at pH 7 was prepared by same method.

4.5 Calcination:

The powder was grinded and was calcined in alumina beaker at 900°C for 2 hours. The calcinations helps in driving out all volatile and gaseous material from powder.

4.6 Phases in calcined powder:

The calcined powder of all composition were subjected to phase analysis by X-ray diffraction

(PW1830 diffractometer ,Phillips,Netherland). This is done to know the different phases present in the calcined powder. The angle range was 15°-70° and scanning rate was.

4.6 Compaction into pellets:

The calcined powder was mixed with 3%PVA solution (for binding). It was mixed in an agate mortar and left to dry. After drying it was scraped and grounded to fine powder. The different composition powder were separately packed after being weighed. The powder was then pressed into pellets by uniaxial compaction with load of 3 ton

4.7 Sintering of pellets:

The compacted bars and pellets were sintered in conventional furnace at 1150°C for 1 hour

4.8 Density of sintered pellets:

The density of the sintered pellets were determined by Archimedes principle using kerosene. The dry weight ,soak weight and suspended weight were measured. The density was calculated by formula:

Density = { dry weight/(soak weight – suspended weight)} *0.81

4.9 Microstructural analysis by SEM

The sintered pellets were taken for SEM analysis. The pellets were sputtered in a sputtering unit. Then they were loaded for analysis. This analysis helps us to know the complete microstructure of the sintered sample

[pic]

Figure 7: Flowchart of the procedure

5. Results and Discussions:

5.1 XRD analysis :

5.1.1 XRD plot of 0.92 BNT- 0.08 BF prepared at different pH





Figure 8(a) and 8(b): XRD plot of 0.92BNT-0.08BF prepared at different pH

Figure 8 shows the XRD plot of 0.92BNT0.08BF prepared at pH value 5-11 and calcined at 900°C. It has been observed that for pH 5 and pH 7 there is no peak shift but for pH 9 peak shifted to the lower value whereas at pH 11 peak shifted to higher value.

5.1.2 XRD plot of 0.94 BNT- 0.06 BF prepared at different pH:

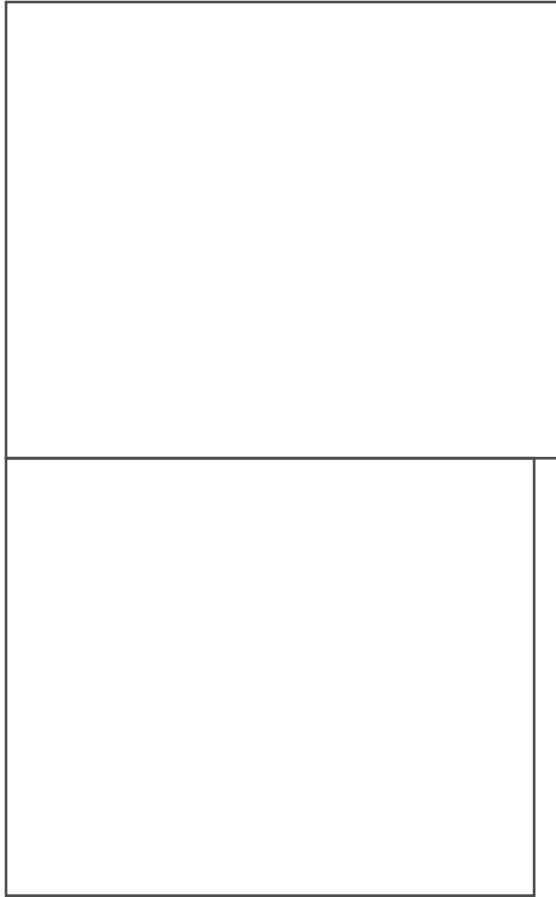
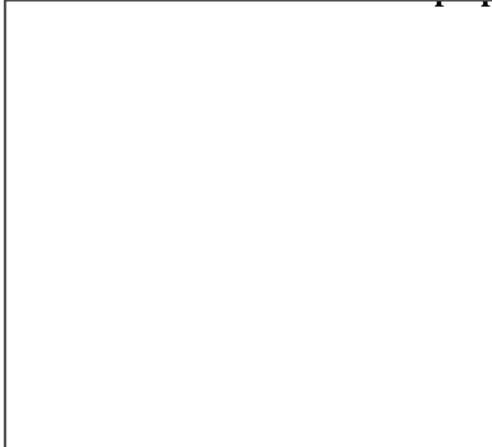


Figure 9(a) and 9(b) : XRD plot of 0.94BNT-0.06BF prepared at different pH

For the sample 0.94 BNT- 0.06 BF the peak shifted to higher values when pH changes from 5 to 7.No effect for pH change for 7,9,11.

5.1.3 XRD of 0.96BNT -0.04BF prepared at different pH:



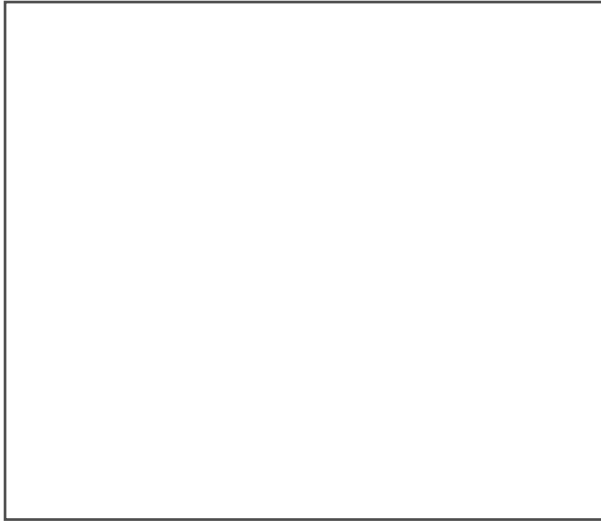


Figure 10(a) and 10(b): XRD of 0.96BNT- 0.04BF prepared at different pH

For the sample 0.96BNT- 0.04BF the peak shifted to lower value when pH changes from 5-7. Furthermore, peak shifted when pH value increased from 7 and there is no peak shift at pH 9 and 11.

5.1.4 XRD of all samples at pH 7:

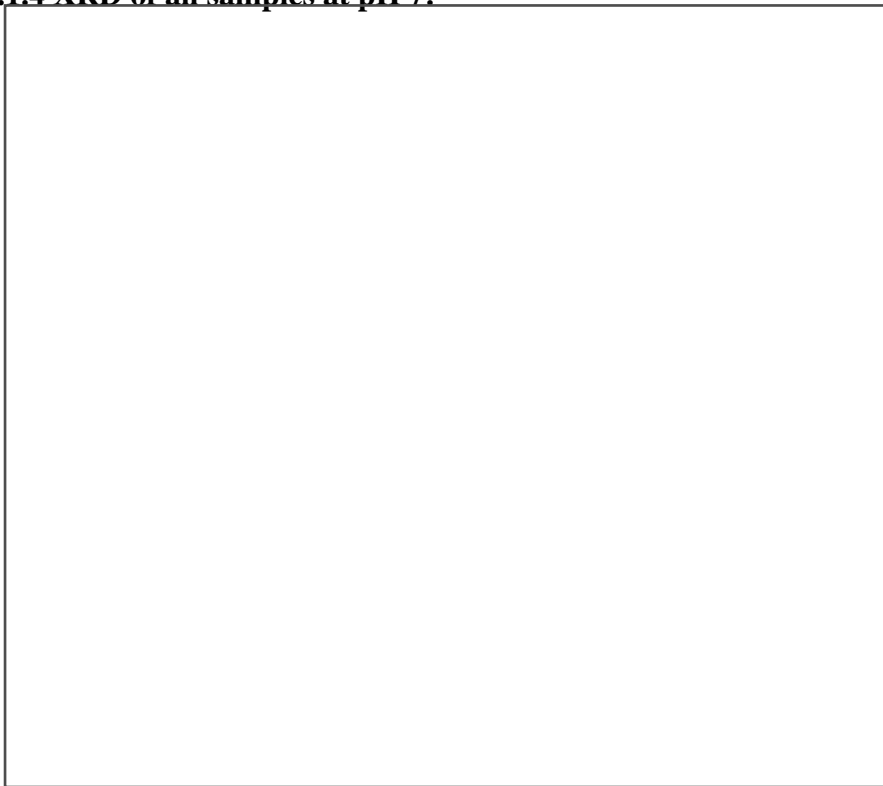


Figure 11: XRD peak of pure BNT with various amount of BF doping at pH 7.

5.2 Crystallite Size:

Table shows the variation of crystallite sizes along with variation in pH value for sample.

Table 2:Crystallite size of the samples.

Sample Name		Crystallite Size
		in nm
0.92 BNT -0.08 BF	pH 5	37.5898
	pH 7	36.3314
	pH 9	34.8304
0.94 BNT-0.06 BF	pH11	33.9130
	pH 5	54.4144
	pH 7	39.9999
0.96 BNT -0.04 BF	pH 9	37.4129
	pH 11	54.5875
	pH 5	42.2668
	pH 7	35.9764
	pH 9	42.5048
	pH 11	38.5601

5.3 Density of sintered pellets:

Density was measured by Archimedes principle. It has been observed that from relative density that 0.94BNT-0.08BF achieve 90-95 % at 1150°C. Whereas for other samples the relative density varies from 85-90%.

Table 3: Density measurement of sintered pellets:

Sample Name		Relative Density(%)
0.92 BNT -0.08 BF	pH 5	88
	pH 7	85
	pH 9	89
	pH 11	87
0.94 BNT-0.06 BF	pH 5	95
	pH 7	90
	pH 9	93
	pH 11	91
0.96 BNT -0.04 BF	pH 5	88
	pH 7	85
	pH 9	89
	pH 11	86

5.4 SEM Analysis:

5.4.1: SEM of calcined powder and sintered pellets of 0.92BNT-0.08BF

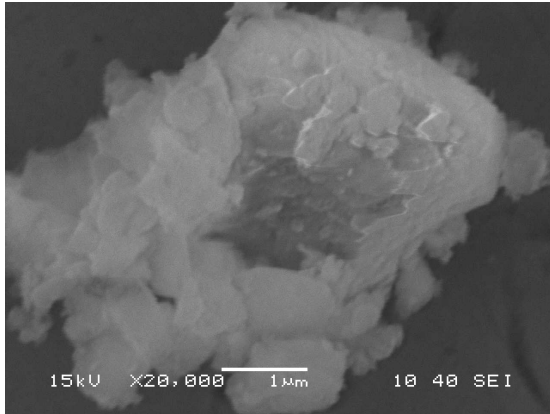


Figure 12: SEM of 0.92BNT-0.08BF calcined powder

From SEM observation it has been found that the powder it has been found that powders are mostly agglomerated and flaky in nature. The figure 12 shows sample 0.92BNT-0.08BF prepared at pH 7.

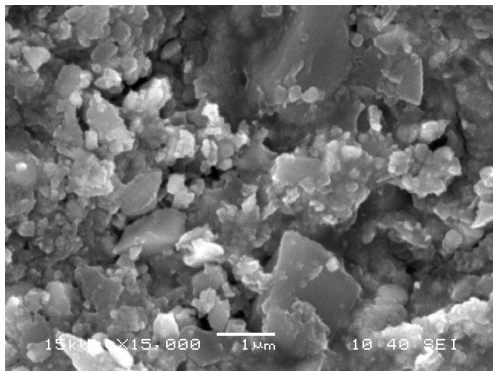


Figure 13: SEM of 0.92BNT-0.08BF sintered pellets

The figure 13 shows SEM micrograph of sintered pellets at 1150°C. SEM micrograph shows there is considerable amount of voids appeared in sintered sample.

5.4.2 SEM of calcined powder and sintered pellets of 0.94BNT-0.06BF:

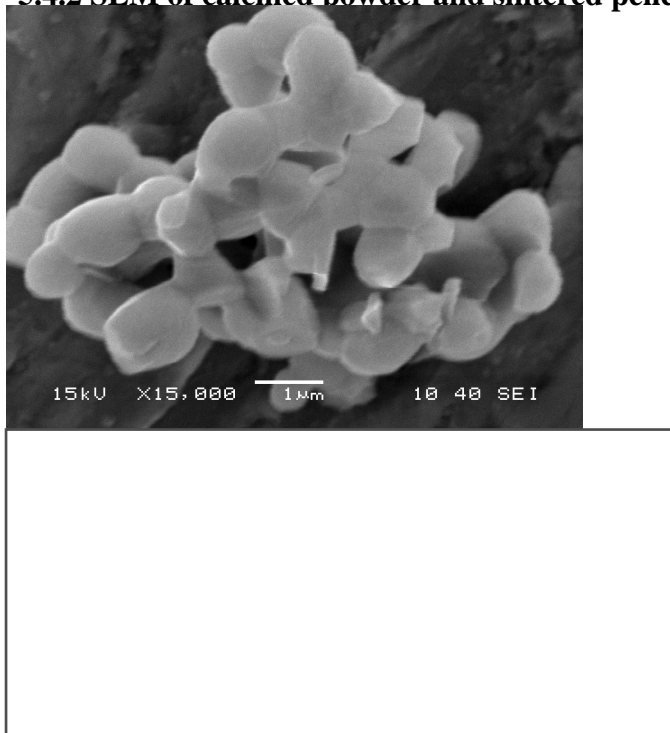


Figure 14: SEM of calcined powder of 0.94BNT-0.06BF

The figure 14 the SEM of powder sample prepared at 900°C. Powders are agglomerated but spherical in shape.

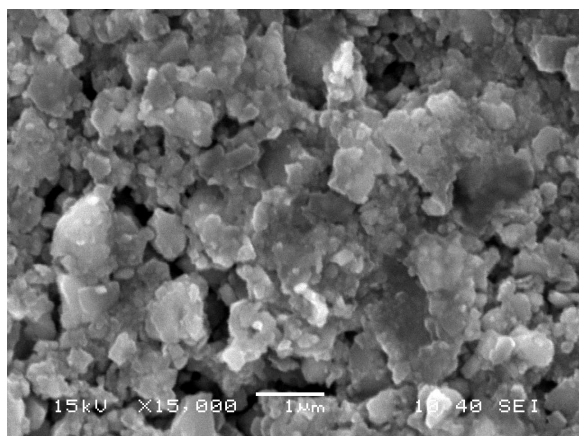




Figure 15: SEM of sintered pellets of 0.94BNT-0.06BF

26

5.4.3 SEM of 0.96BNT-0.04BF sintered pellets:

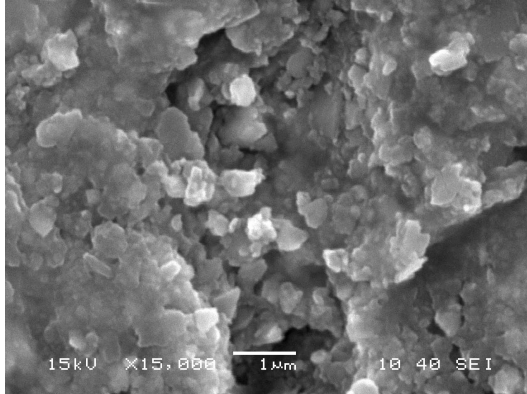


Figure 16: SEM of 0.96BNT-0.04BF sintered pellets

6. Conclusion:

(1-x) BNT-x BF powder was successfully synthesized at 900°C. The variation in pH shows different crystallite size. The crystallite size decreases in a regular manner for sample 0.92BNT-0.08BF with increase in pH value. For sample 0.94BNT-0.06BF Crystallite size decreases at pH from 5 to 9. Then it increases drastically. For sample 0.96 BNT-0.04BF the variation is not regular.

The relative density for 0.94BNT-0.06BF has been achieved up to 90-95% when samples were sintered at 1150°C. but for other samples density was not more than 90% at same temperature. So it can be concluded for preparation of (1-x)BNT-xBF the pH should be varied between 7 to 9 for auto-combustion synthesis and sample should be sintered between 1150°C -1250°C.

References:

1. Dielectric properties of some low-lead or lead-free perovskite-derived materials: $\text{Na}_{0.5}\text{Bi}_{0.5}\text{TiO}_3\text{--PbZrO}_3$, $\text{Na}_{0.5}\text{Bi}_{0.5}\text{TiO}_3\text{--BiScO}_3$ and $\text{Na}_{0.5}\text{Bi}_{0.5}\text{TiO}_3\text{--BiFeO}_3$ ceramics P. Marchet, E. Boucher, V. Dorcet, J.P. Mercurio.
2. Structural and dielectric studies of the $\text{Na}_{0.5}\text{Bi}_{0.5}\text{TiO}_3\text{--BiFeO}_3$ system V. Dorcet, P. Marchet*, G. Trolliard.
3. Takenaka, T., Sakata, K. and Toda, K., *Ferroelectrics*, 1990, 106, 375.
4. Takenaka, T., Okuda, T. and Takegahara, K., *Ferroelectrics*, 1997, 196, 175.
5. Nagata, H. and Takenaka, T., *Jpn. J. Appl. Phys.*, 1998, 37(9B), 5311.
6. Herabut, A. and Safari, A., *J. Am. Ceram. Soc.*, 1997, 80, 2954.
7. Wang, T. B., Gao, M., Wang, L. E., Lu, Y. K. and Zhou, D. P., *J. Inorg. Mater.*, 1997, 2, 223.
8. Kuharungrong, S. and Schulze, W., *J. Am. Ceram. Soc.*, 1996, 79, 1273.
9. Sakata, K. and Masuda, Y., *Ferroelectrics*, 1974, 7, 347.
10. Saad, S. and Mercurio, J.-P., *J. Eur. Ceram. Soc.*, 2001, 21, 1333.
11. Gomah-Petry, J. R., Salak, A. N., Marchet, P., Ferreira, V. M. and Mercurio, J.-P., *Phys. Status Solidi B*, 2004, 241(8), 1949.
12. Cross, L. E., Jang, S. J. and Newnham, R. E., Large electrostrictive effects in relaxor Ferroelectrics. *Ferroelectrics*, 1980, 23, 187–192.
13. Nomura, S. and Uchino, K., Recent applications of PMN-based electrostrictors. *Ferroelectrics*, 1983, 50, 197–202.
14. Uchino, K., *Ferroelectric Devices*. Marcel Dekker, Inc., New York, 2000.
15. Sodium-bismuth titanate based lead-free ferroelectric materials Jean-Richard Gomah-Petry, Senda Saad, Pascal Marchet, Jean-Pierre Mercurio
16. H. Nagata and T. Takenaka, "Lead-Free Piezoelectric Ceramics of $(\text{Bi}_{0.5}\text{Na}_{0.5})\text{TiO}_3\text{--}0.5(\text{Bi}_2\text{O}_3\text{--Sc}_2\text{O}_3)$ System," *Jpn. J. Appl. Phys.*, **36** [9B] 6055-7 (1997).
17. A.J. Moulson and J.M. Herbert, *Electroceramics: Materials, Properties, Applications.*, 2nd ed. Wiley and Sons, West Sussex, England, 2003.
18. A.N. Soukhovak, H. Wang, G.W. Farrey, and Y.-M. Chiang, "Superlattice in Single Crystal

Barium- Doped Sodium Bismuth Titanate," *J. Phys. Chem. Solids*, **61** [2] 301-4 (2000).

19. G.O. Jones and P.A. Thomas, "Investigation of the Structure and Phase Transitions in the Novel A-site Substituted Distorted Perovskite Compound $\text{Na}_{0.5}\text{Bi}_{0.5}\text{TiO}_3$," *Acta Crystallogr.*, **B 58** [2] 168-78 (2002).
20. P. Woodward, "Octahedral Tilting in Perovskites. I. Geometrical Considerations, *Acta Crystallogr.*, **B 53** [1] 32-43 (1997).
21. J.A. Zvirgzds, P.P. Kapostins, J.V. Zvirgzde, and T.V. Krunzina, "X-Ray Study of Phase Transitions in Ferroelectric $\text{Na}_{0.5}\text{Bi}_{0.5}\text{TiO}_3$," *Ferroelectrics*, **40** [1-2] 75-7 (1982).
22. S.-E. Park and K.S. Hong, "Variations of Structure and Dielectric Properties on Substituting A-site Cations for Sr^{2+} in $(\text{Na}_{1/2}\text{Bi}_{1/2})\text{TiO}_3$," *J. Mater. Res.*, **12** [8] 2152-7 (1997).

23. K. Sakata and Y. Masuda, "Ferroelectric and Antiferroelectric Properties of (Na_{0.5} Bi_{0.5}) TiO₃-SrTiO₃ Solid Solution Ceramics," *Ferroelectrics*, **7** [1-4] 347-9 (1974).
24. S. Said, P. Marchet, T. Merle-Mejean, and J.-P. Mercurio, "Raman Spectroscopy Study of the Na_{0.5}Bi_{0.5}TiO₃-PbTiO₃ System," *Mater. Lett.*, **58** [9] 1405-9 (2004).
25. J.-K. Lee, J.Y. Yi, and K.-S. Hong, "Relationship Between Structure and Dielectric Property in (1-x)(Na_{1/2}Bi_{1/2})TiO₃ - xPbZrO₃ Ceramics," *Jpn. J. Appl. Phys., Part 1*, **40** [10] 6003-7 (2001).
26. I.P. Pronin, P.P. Syrnikov, V.A. Isupov, V.M. Egorov, N.V. Zaitseva, and A.F. Ioffe, "Peculiarities of Phase Transitions in Sodium-Bismuth Titanate," *Ferroelectrics*, **25** [1-4] 395-7 (1980).
27. P. Woodward, "Octahedral Tilting in Perovskites. II. Structure Stabilizing Forces, " *Acta Crystallogr.*, **B 53** [1] 44-66 (1997).
28. G.O. Jones and P.A. Thomas, "The Tetragonal Phase of Na_{0.5}Bi_{0.5}TiO₃ - a New Variant of the Perovskite Structure," *Acta Crystallogr.*, **B 56** [3] 426-30 (2000).
29. M.E. Lines and A.M. Glass, *Principles and Applications of Ferroelectrics and Related Materials*. Oxford University Press, New York, 2001.
30. S.A. Sheets, A.N. Soukhovjak, N. Ohashi, and Y.-M. Chiang, "Relaxor Single Crystals in the (Bi_{1/2}Na_{1/2})_{1-x}Ba_xZr_yTi_{1-y})₃ System Exhibiting High Electrostrictive Strain," *J. Appl. Phys.*, **90** [10] 5287-95 (2001).
31. S. Kuharuangrong, "Studies on the Dielectric Properties and the Phase Transitions of the Bi_{0.5}Na_{0.5}TiO₃ PbTiO₃"; Ph. D. Thesis. Alfred University, Alfred, NY, 1994.

32. T. Takenaka, K.-I. Maruyama, and K. Kakata, "(Bi_{0.5} Na_{0.5})TiO₃-BaTiO₃ System for Lead-Free Piezoelectric Ceramics," *Jpn. J. Appl. Phys.*, **30** [9B] 2236-9 (1991).
33. H.-D. Li, C.-D. Feng, and W.-L. Yao, "Some Effects of Different Additives on Dielectric and Piezoelectric Properties of (Bi_{1/2}Na_{1/2})TiO₃-BaTiO₃ Morphotropic-Phase-Boundary Composition," *Mater. Lett.*, **58** [7-8] 1194-8 (2004).
34. J.-R. Gomah-Petry, S. Said, P. Marchet, and J.-P. Mercurio, "Sodium-Bismuth Titanate Based Lead-Free Ferroelectric Materials," *J. Eur. Ceram. Soc.*, **24** [6] 1165-9 (2004).
35. J. Suchanicz, M.G. Gavshin, A.Y. Kudzin, and C. Kus, "Dielectric Properties of (Na_{0.5}Bi_{0.5})_{1-x} MexTiO₃ Ceramics near Morphotropic Phase Boundary," *J. Mater. Sci.*, **36** [8] 1981-5 (2001).
36. S. Said and J.-P. Mercurio, "Relaxor Behavior of Low Lead and Lead Free Ferroelectric Ceramics of the Na_{0.5}Bi_{0.5}TiO₃-PbTiO₃ and Na_{0.5}Bi_{0.5}TiO₃- K_{0.5}Bi_{0.5}TiO₃ Systems," *J. Eur. Ceram. Soc.*, **21** [10-11] 1333-6 (2001).
37. S. Kuharuangrong, "Effect of La and K on The Microstructure and Dielectric Properties of Bi_{0.5}Na_{0.5}TiO₃-PbTiO₃," *J. Mater. Sci.*, **36** [7] 1727-33 (2001).
38. H. Nagata, M. Yoshida, Y. Makiuchi, and T. Takenaka, "Large Piezoelectric Constant and High Curie Temperature of Lead-Free Piezoelectric Ceramic Ternary System Based on Bismuth Sodium Titanate-Bismuth Potassium Titanate- Barium Titanate Near the Morphotropic Phase Boundary," *Jpn. J. Appl. Phys.*, **42**[12] 7401-3 (2003).
39. A. Sasaki, T. Chiba, Y. Mamiya, and E. Otsuki, "Dielectric and Piezoelectric Properties of (Bi_{0.5}Na_{0.5})TiO₃-(Bi_{0.5}K_{0.5})TiO₃ Systems," *Jpn. J. Appl. Phys., Part1*, **38** [9B] 5564-7 (1999).

40. H. Ishii, H. Nagata, and T. Takenaka, "Morphotropic Phase Boundary and Electrical Properties of Bisumuth SodiumTitanate - Potassium Niobate Solid- Solution Ceramics," *Jpn. J. Appl. Phys., Part 1*, **40** [9 B] 5660-3 (2001).
41. H. Nagata and T. Takenaka, "Lead-Free Piezoelectric Ceramics of $(\text{Bi}_{0.5}\text{Na}_{0.5})\text{TiO}_3\text{-KNbO}_3\text{-}0.5(\text{Bi}_2\text{O}_3\text{-Sc}_2\text{O}_3)$ System," *Jpn. J. Appl. Phys.*, **37** [9B] 5311-4 (1998).
42. A. Herabut and A. Safari, "Processing and Electromechanical Properties of $(\text{Bi}_{0.5}\text{Na}_{0.5})(1\text{-}1.5\text{x})\text{La}_x\text{TiO}_3$ Ceramics," *J. Am. Ceram. Soc.*, **80** [12] 2954-8 (1997).
43. J.Y. Yi, J.-K. Lee, and K.-S. Hong, "Dependence of the Microstructure and the

31

- Electrical Properties of Lanthanum-Substituted $(\text{Na}_{1/2}\text{Bi}_{1/2})\text{TiO}_3$ on Cation Vacancies," *J. Am. Ceram. Soc.*, **85** [12] 3004-10 (2002).
44. M. Aparna, T. Bhimasankaram, G.S. Kumar, and G. Prasad, "Synthesis and Characterization of Lanthanum Doped Sodium Bismuth Titanate," *Modern Physics Letters*, **B 16** [26] 1007-19 (2002).
 45. X.X. Wang, K.W. Kwok, X.G. Tang, H.L.W. Chan, and C.L. Choy, "Electromechanical Properties and Dielectric Behavior of $(\text{Bi}_{1/2}\text{Na}_{1/2})(1\text{-}1.5\text{x})\text{Bi}_x\text{TiO}_3$ Lead-Free Piezoelectric Ceramics," *Solid State Commun.*, **129** [5] 319-23 (2004).
 46. H. Nagata and T. Takenaka, "Additive Effects on Electrical Properties of $(\text{Bi}_{1/2}\text{Na}_{1/2})\text{TiO}_3$ Ferroelectric Ceramics," *J. Eur. Ceram. Soc.*, **21** [10-11] 1299-302 (2001).
 47. J.P. Attfield, "'A' Cation Control of Perovskite Properties," *Cryst. Eng.*, **5** [3-4] 427-38 (2002).
 48. C.A. Randall, A.S. Bhalla, T.R. Shrout, and L.E. Cross, "Classification and Consequences of Complex Lead Perovskite Ferroelectrics with Regard to B-site Cation Order," *J. Mater. Res.*, **5** [4] 829-34 (1990).
 49. W.A. Schulze, Thesis Discussion, Alfred University, 2002-2004.
 50. Y.J. Feng, Z. Xu, and X. Yao, "Effect of Sn Doping on the Phase Transition Behaviors of Antiferroelectric Lead Zirconate Titanate," *Mater. Sci. Eng.*, **B 99** [1-3] 499-501 (2003).
 51. B. Jaffe, W.R.C. Jr., and H. Jaffe, *Piezoelectric Ceramics*. Academic Press Limited, New York, 1971.
 52. S. Kuharuangrong and W. Schulze, "Characterization of $\text{Bi}_{0.5}\text{Na}_{0.5}\text{TiO}_3\text{-PbTiO}_3$ Dielectric Materials," *J. Am. Ceram. Soc.*, **79** [5] 1273-80 (1996)

Mixed solution.

Combustion on hot plate

Formation of a fluffy mass

Grinding of the powder

XRD analysis

Addition of 3%PVA

Compaction of powder into pellets

Density measurement

Sintering at 1150oC for 1 hour

Calcination at 900oC for 2 hours

$\text{Bi}(\text{NO}_3)_3 \cdot 5\text{H}_2\text{O} + \text{NaNO}_3$

$\text{Fe}(\text{NO}_3)_3$ solution

SEM analysis

$\text{Bi}(\text{NO}_3)_3 \cdot 5\text{H}_2\text{O}$

Ti-Nitrate solution.